The Oriented γ Form of Isotactic Polypropylene

Finizia Auriemma,* Claudio De Rosa, Tiziana Boscato, and Paolo Corradini

Dipartimento di Chimica, Università degli studi di Napoli "Federico II", Complesso Monte Sant' Angelo, Via Cintia, 80126 Napoli, Italy

Received January 10, 2001; Revised Manuscript Received March 23, 2001

ABSTRACT: A structural analysis of the oriented γ form of isotactic polypropylene (iPP) is presented. The X-ray diffraction intensity distribution in the oriented γ form is quantitatively evaluated for the first time. The structural analysis is performed on a new, poorly stereoregular ([*mmmm*] = 35%) polypropylene material, prepared with a novel C_2-symmetric zirconocene based catalytic system, showing elastomeric properties. The sample, initially amorphous, partially crystallizes upon aging. In the oriented crystalline materials, obtained by stretching the aged sample, the crystallites tend to assume a preferred orientation with the chain axes parallel to the draw direction. Disorder is present in the structure. For low draw ratios (less than twice the initial length) disordered crystalline modifications, very close to the γ form of iPP, are obtained; increasing the draw ratio, crystalline modifications, closer to the α form of iPP, are observed. The structural disorder occurring in our stretched samples originates from the random succession of bilayers of chains with chains parallel (like in the α form) or tilted ≈81° each other (like in the γ form). The results of this analysis are the follows. For the sample stretched at a low draw ratio, ≈75% of the bilayers of chains are faced each other like in the γ form so that the fraction of bilayers with chain axes pointing preferentially along the draw direction is on the order of 60−65% (the remaining 35−40%, being oriented with the chain axes tilted ≈81° to the draw direction). For the samples stretched at higher draw ratios, the fraction of bilayers facing each other like in the γ form is reduced to 20−30%, so that only 10−15% of the bilayers results oriented with the chain axes nearly normal to the draw direction. This is as if, in all cases, the regions of the crystals with chains arranged like in the α form tend to be oriented with the chain axes parallel to the stretching direction rather than tilted ≈81°. A *continuum* of disordered modifications intermediate between the pure γ and α forms could exist. The possible inclusion in the crystalline domains of stereo defects (mainly of the kind *mrrm*), which would favor the γ -like packing situations on the local scale, is discussed.

Introduction

The γ form of isotactic polypropylene (iPP) has been considered as a rare, rather exotic polymorph for years: with iPP samples prepared using heterogeneous Ziegler−Natta catalysts, the γ form may be obtained only by crystallization at high pressures (about 5000 atm), or at atmospheric pressure of very low molecular weight samples and copolymers containing small amounts (in the range 5−20 mol %) of other 1-olefins.[1] Commercial iPP, indeed, under the most common conditions of crystallization, gives the α form. For high molecular weight iPP samples prepared with metallocene catalysts, the γ form crystallizes more easily even at atmospheric pressure.[2−4] It has been shown that the content of γ phase in these sample seems to be strictly related to the average length of fully isotactic sequences.[4]

The polymorphic behavior of iPP, with respect to the relative stability of the γ and the α forms, has been essentially studied only in the case of unoriented powder samples, so far. Uniaxial drawing procedures of iPP samples generally produce the α form.[1] In 1966, a paper appeared in the literature showing that the γ form of iPP may be obtained also in uniaxially oriented specimens, in the case of low molecular weight iPP samples.[5] As pointed out in ref 5, the X-ray fiber diffraction patterns of oriented specimens of iPP in the γ form are very similar to those of uniaxially oriented samples of iPP crystallized in the α form containing a non-negligible portion of daugther lamellae, tilted by ≈81° with respect to the parent lamellae, the parent lamellae being oriented with the *c* axes parallel to the stretching direction, the daughter lamellae having the *a* axes parallel to the *c* axis of the parent ones.[6−9] The only difference is the presence in the fiber pattern of the γ form, of an equatorial reflection at d = 4.42 Å (2θ = 20.1°).

Nowadays, using particular metallocene catalysts based on C_2-symmetric zirconocene systems, high molecular weight polypropylenes, with a low *mmmm* pentad content and a random distribution of defects, showing interesting elastomeric properties may be produced.[10] These materials crystallize prevailingly in the γ form; if stretched, the γ form becomes oriented[10] and does not transform itself into the α form, provided that the draw ratio is low. In this paper, we present for the first time a quantitative interpretation of the X-ray fiber diffraction patterns of such stretched polypropylene showing the oriented γ form. An analysis of the structural disorder present in the γ form will be presented.

Structural Considerations

The structural model of the γ form of iPP is characterized by a nonparallel arrangement of the chains within the unit cell, and represents a rare example of molecular architecture in the crystals of synthetic polymers.[11,12] The chains, in a 3-fold helical conformation, lie parallel to both diagonals in the $a_\gamma - b_\gamma$ plane of the orthorhombic unit cell proposed by Brückner and Meille[11] (a_γ = 8.54 Å, b_γ = 9.93, c_γ = 42.41 Å) which hence measure $|\mathbf{a}_\gamma + \mathbf{b}_\gamma| = |\mathbf{a}_\gamma - \mathbf{b}_\gamma|$ = 13.08 Å, that is, twice the helical periodicity. The chain axes (along the two diagonals) form an angle of 81.4°, a value which is close to that one formed by chain axes in branching of

10.1021/ma0100504 CCC: $20.00
Published on Web 06/06/2001

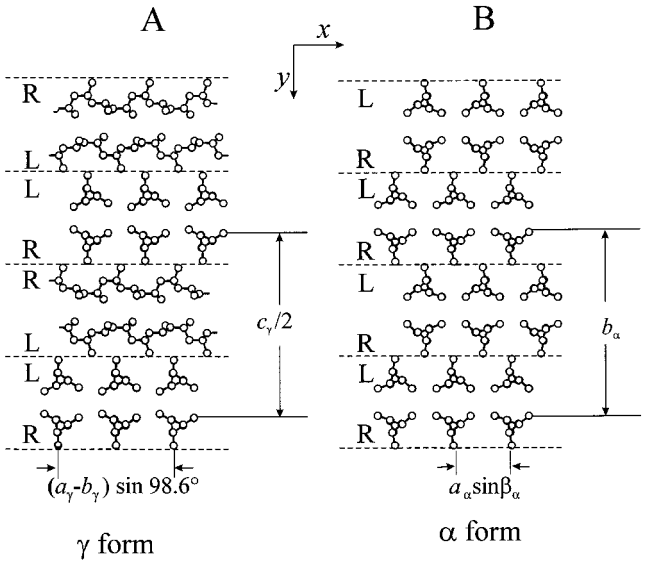

Figure 1. Models of packing proposed for the γ (A) and the α (B) forms of iPP. The dashed horizontal line delimit bilayers of chains. Subscripts γ and α identify unit cell parameters referred to the orthorhombic and monoclinic unit cells of the γ[11] and α[15] forms, respectively. R and L identify rows of all right- and all left-handed helices, respectively.

α-iPP crystals.[8,9] The proposed space group is *Fddd*. It is consistent with the random substitution in the same lattice position of coaxial, isomorphous and anticlined chains, i.e., of chains having opposite orientation as far as the C−C bonds connecting the methyl groups to the chain backbone, pointing all upward (up) or downward (down) an oriented direction parallel to the chain axes.[13] The projection of the structural model proposed for the γ form of iPP, in a plane perpendicular to one diagonal (i.e., $\mathbf{a}_\gamma + \mathbf{b}_\gamma$), which allows for helices tilted ≈81° each other to be clearly distinguished, is shown in Figure 1A. The projection in the plane $a_\alpha(\sin \beta_\alpha) - b_\alpha$ of the structural model of the α form of iPP is shown for comparison in Figure 1B (unit cell parameters $a_\alpha = 6.65$ Å, $b_\alpha = 20.73$ Å, $c_\alpha = 6.50$ Å $\beta_\alpha = 98.67°$);[14−16] in both cases, for clarity, coaxial anticlined helices are omitted from the drawing.

There are strong analogies in the packing mode of the helices in the α and γ polymorphs. In both forms, the chains are in the 3/1 helical conformation (chain periodicity ≈6.5 Å), and are organized in double layers piled along the b_α axis direction in the α form, along the c_γ axis direction ($c_\gamma \approx 2b_\alpha$) in the γ form (see Figure 1). If we orient the structural models of the γ and α forms as in Figure 1, with c_γ parallel to b_α and the diagonal $a_\gamma + b_\gamma$ ([110] lattice direction) parallel to $\mathbf{c}_\alpha$ we also notice that the direction of the diagonal $a_\gamma - b_\gamma$ ([$\bar{1}$10] lattice direction) also becomes nearly coincident with the directions of lattice parameters a_α, the diagonals $a_\gamma + b_\gamma$ and $a_\gamma - b_\gamma$ forming an angle of 98.6° (or 81.4°), which nearly coincides with β_α. Within the bilayers, chains of opposite chirality are related by a glide plane symmetry in both crystalline forms. The up/down disorder is a structural feature which characterizes both the α and γ modifications.[14−17] Furthermore, the ≈81° tilt between adjacent bilayers is a feature of the regular crystallographic structure of γ form and it has been observed in branching crystals of the α form, at the interface between regular domains of all parallel chains diffracting incoherently.[6−9] In the γ form, as well as at the interface between the tilted lamellae in the α form, consecutive bilayers of chains are faced through isomorphous chains, whereas the α form of iPP is characterized by the regular alternation of rows of enantiomorphous helices along the b_α axis direction. We also notice that in the α form, the values of the unit cell parameters a_α and c_α are very similar.

Table 1. Bragg Distances (*d*), Bragg Angles (2*θ*, Cu Kα), and Cylindrical Coordinates ξ and ζ of the Main *hkl* Reflections, Calculated for the γ Form of IPP[a]

	γ form			
$(hkl)_\gamma$	d (Å)	ξ (Å^{-1})	ζ (Å^{-1})	2θ (deg)
	Equator			
111	6.40	0.156	0	13.8
113	5.89	0.170	0	15.0
008	5.30	0.189	0	16.7
115	5.15	0.194	0	17.2
117	4.42	0.226	0	20.1
00 12	3.53	0.283	0	25.2
1,1,11	3.31	0.302	0	26.9
220	3.24	0.309	0	27.5
222	3.20	0.312	0	27.9
224	3.10	0.322	0	28.8
226	2.94	0.340	0	30.4
1,1,15	2.59	0.386	0	34.5
333	2.13	0.469	0	42.4
1,1,19	2.11	0.474	0	42.8
335	2.09	0.478	0	43.2
	First Layer Line			
111	6.40	0.030	0.153	13.8
113	5.89	0.073	0.153	15.0
115	5.15	0.120	0.153	17.2
117	4.42	0.167	0.153	20.1
202	4.19	0.183	0.153	21.2
026	4.06	0.193	0.153	21.9

[a] The $(hkl)_\gamma$ Miller indices are referred to the orthorhombic unit cell of the γ form ($a_\gamma = 8.54$ Å, $b_\gamma = 9.93$ Å, $c_\gamma = 42.41$ Å).[11] For the cylindrical coordinates, the γ crystallites are supposed to assume a preferred orientation with the diagonals $\mathbf{a}_\gamma + \mathbf{b}_\gamma$ or $\mathbf{a}_\gamma - \mathbf{b}_\gamma$ of the orthorhombic unit cell parallel to the draw direction; these diagonal directions correspond to the chain axes directions.

As we shall see, uniaxially drawing procedures of the polypropylene sample under examination lead the γ form to assume a preferred orientation with the diagonals in the $a_\gamma b_\gamma$ plane of the orthorhombic unit cell parallel to the fiber axis. For a ready interpretation of the X-ray fiber diffraction diagrams of such sample, the cylindrical coordinates ξ and ζ of the oriented γ form for the main *hkl* reflections are reported in Table 1 together with the Bragg distances (d) and the 2θ (Cu Kα) diffraction angles. For comparison, the main reflections along the equator and the first layer line for the α form are listed in Table 2, in two cases: when the α crystallites are oriented with the chain axes parallel to the stretching direction as well as for the ≈81° tilted α lamellae, where the crystallites are oriented with the a_α axes parallel to the fiber axis direction. Of course, for the tilted α domains, (see Table 2) the $(hk0)_\alpha$ reflections disappear from the equator and appear on the h-th layer line (for instance the $(110)_\alpha$ and the $(130)_\alpha$ would appear on the first layer line at $\xi = 0.043$ and 0.143 Å^{-1}, respectively), the reflections of the class $(0kl)$ become equatorial (as for instance the $(041)_\alpha$, $(061)_\alpha$ and $(042)_\alpha$ occurring at $\xi = 0.246$, 0.324 and 0.366 Å^{-1}, respectively) whereas those with Miller indices (hkl) with $|h| = |l|$ are left unaltered in the same position (and with the same intensity) as those relative to the α domains with a c axis orientation (for instance the $(040)_\alpha$, $(111)_\alpha$, and $(\bar{1}31)_\alpha$. reflections). The intensity distribution in the case of the oriented pure γ form

Table 2. Bragg Distances (d), Bragg Angles (2θ, Cu Kα) and Cylindrical Coordinates ξ and ζ of the Main hkl Reflections, Calculated for the α Form of IPP[a]

α Form, *c*-Axis Orientation

$(hkl)_\alpha$	d (Å)	ξ (Å^{-1})	ζ (Å^{-1})	2θ (deg)
		Equator		
110	6.25	0.160	0	14.2
040	5.18	0.193	0	17.1
130	4.76	0.210	0	18.6
{150				
{060	3.46	0.289	0	25.7
{200				
{210	3.28	0.305	0	27.2
220	3.13	0.319	0	28.5
		First Layer Line		
111	4.18	0.181	0.154	21.1
{$\bar{1}$31				
{041	4.06	0.191	0.154	21.8

α Form, *a*-Axis Orientation

	α form			
$(hkl)_\alpha$	d (Å)	ξ (Å^{-1})	ζ (Å^{-1})	2θ (deg)
		Equator		
040	5.18	0.193	0	17.1
041	4.07	0.246	0	21.8
060	3.46	0.289	0	25.7
061	3.09	0.324	0	28.9
042	2.73	0.366	0	32.8
		First Layer Line		
110	6.25	0.043	0.154	14.2
130	4.76	0.143	0.154	18.6
111	4.21	0.181	0.154	21.1
$\bar{1}$31	4.07	0.191	0.154	21.8

[a] The $(hkl)_\alpha$ Miller indices are referred to the monoclinic unit cell of the α form (a_α = 6.65 Å, b_α = 20.73 Å, c_α = 6.50 Å, β_α = 98.67°).[15] Two limit cases of preferred orientations of the crystals are considered, the c_α axes are parallel to the draw direction (c_α axis orientation) and the a_α axes are parallel to the draw direction (a_α axis orientation).

would show features which are somehow intermediate between those calculated for α lamellae *c*-axis and *a*-axis oriented (see Table 1). Also in this case, indeed, some reflections split in two contributions. More precisely the $(hkl)_\gamma$ reflections with $h = k \neq 0$ are apparent both on the equatorial and on the *k*-th layer line, (for instance the $(111)_\gamma$, $(113)_\gamma$, $(115)_\gamma$, $(117)_\gamma$, etc.), whereas the reflections with h and/or $k = 0$ (like for instance the $(008)_\gamma$, $(00\ 12)_\gamma$, $(202)_\gamma$, and $(026)_\gamma$ are not split and appear on the $(h + k)_\gamma$/2th layer line. Observe that these latter reflections would be equivalent, as far as the position (and the intensity) to the $(040)_\alpha$, $(060)_\alpha$, $(111)_\alpha$, and $(\bar{1}31)_\alpha$. reflections in the pure α form, whatever the orientation of the chains.

Experimental Section

The elastomeric polypropylene sample here examined (PP) was prepared with the novel metallocene catalytic system *rac*-methylene bis(3-*i*-propyl-1-indenyl)zirconium dichloride using methylalumoxane (MAO) as cocatalyst as described in ref 10 (M_w = 143700, [*mmmm*] = 35%, sample 8 of ref 10). The distribution of steric errors is nearly random; on this assumption, the average length of fully isotactic sequences amounts to ≈6−7 monomeric units. The as prepared sample is amorphous and partially crystallizes in the γ form upon aging, the degree of crystallinity being 15−20%.[10]

Oriented samples were prepared by stretching strips cut from aged films quenched from the melt in liquid N_2, 0.2 mm thick. The initial gauge length was 5 mm and the width 3 mm. The reported X-ray diffraction patterns are relative to samples stretched 2 (sample A), 4 (sample B), and 6 (sample C) times their initial length (draw ratios λ = final length/initial length = 2, 4, and 6, respectively).

The 2D−X-ray fiber diffraction patterns were obtained on a BAS-MS imaging plate (FUJIFILM) using a cylindrical camera and processed with a digital imaging reader (FUJIBAS 1800; Cu Kα radiation, monochromatized with a graphite single crystal).

X-ray diffraction data were also collected using a Nonius MACH3 (four circles, K geometry) automatic diffractometer, with Cu Kα radiation (monochromatized with a graphite single crystal), always maintaining an equatorial geometry. The reciprocal space along the equator ($\zeta = 0$) and the first layer line ($\zeta = 1/c_\alpha = 0.153$ Å^{-1}) for ξ in the range 0−1 Å^{-1} was sampled at steps of $\xi = 0.0033$ Å^{-1}, ξ and ζ being the cylindrical reciprocal coordinates. X-ray diffraction profiles were also collected along the azimuthal angle χ at fixed values of the 2θ diffraction angle, corresponding to the first strong reflection on the equator, i.e., $(111)_\gamma$ (d = 6.40 Å) for sample A and $(110)_\alpha$ (d = 6.25 Å) for samples B and C. The Lorentz and polarization (Lp) factor, when applied, is, according to the diffraction geometry, $Lp = [(\cos^2 2\theta + \cos^2 2\theta_m)/(1 + \cos^2 2\theta_m)]\text{-}[(1 + \cos 2\theta_m + \cos^2 2\theta)/(1 + \cos 2\theta_m)](2 \sin 2\theta)^{-1}$ with θ_m (=26.6°) being the diffraction angle referred to the Cu Kα radiation of the Bragg planes of the graphite single crystal used as monochromator.

Experimental Results

As already reported in ref 10, the melt quenched specimens of our PP sample, initially amorphous, crystallize upon aging. When the aged sample is stretched, the crystallites tend to assume a preferred orientation with the chain axes parallel to the draw direction. The X-ray diffraction patterns of PP samples stretched at $\lambda = 2$ (sample A) and $\lambda = 6$ (sample C) and kept under tension, are shown in Figure 2, parts a and b, respectively. This material is a thermoplastic elastomer: the stretched sample, if kept for a short time in tension, recovers almost 100% of the initial dimensions, upon release of the stress; samples kept in tension for a time long enough (on the order of several hours), instead, partially lose their elastic properties and become more fragile.[18]

All the stretched samples show crystalline reflections which become progressively less arced with increasing the draw ratio; also, for sample C, the amorphous halo appears slightly polarized on the equator. The Bragg spacings and the intensities of the reflections observed in the X-ray diffraction patterns of samples A and C (Figure 2, parts a and b) are reported in Table 3. They nearly correspond to the same fiber axis period of ≈6.53 Å. Also, the position of the most intense reflections are nearly coincident within the experimental error for the two samples, except for the position of the third reflection along the equator (arrowed in Figure 2) which are observed at d = 4.44 Å (2θ = 20.0°, Cu Kα) in the case of sample A (Figure 2a) at d = 4.80 Å (2θ = 18.4°, Cu Kα) in the case of sample C (Figure 2b).

For sample A, all the observed reflections may be interpreted in terms of the orthorhombic structural model of the γ form of iPP, if we assume that the diagonals of the orthorhombic unit cell (corresponding to the direction of one-half of the chain axes) are preferentially oriented parallel to the draw direction. The three strongest equatorial reflections at d = 6.41, 5.51, and 4.44 Å are hence indexed as $(111)_\gamma$, $(008)_\gamma$, and $(117)_\gamma$, respectively; along the first layer line the nearly meridional reflection (labeled with "m" in Figure 2a) corresponds to the $(111)_\gamma$ whereas the second broad maximum, occurring at $d \approx 4.18$ Å, correspond to the reflections $(202)_\gamma + (026)_\gamma$ (see Table 3). Therefore,

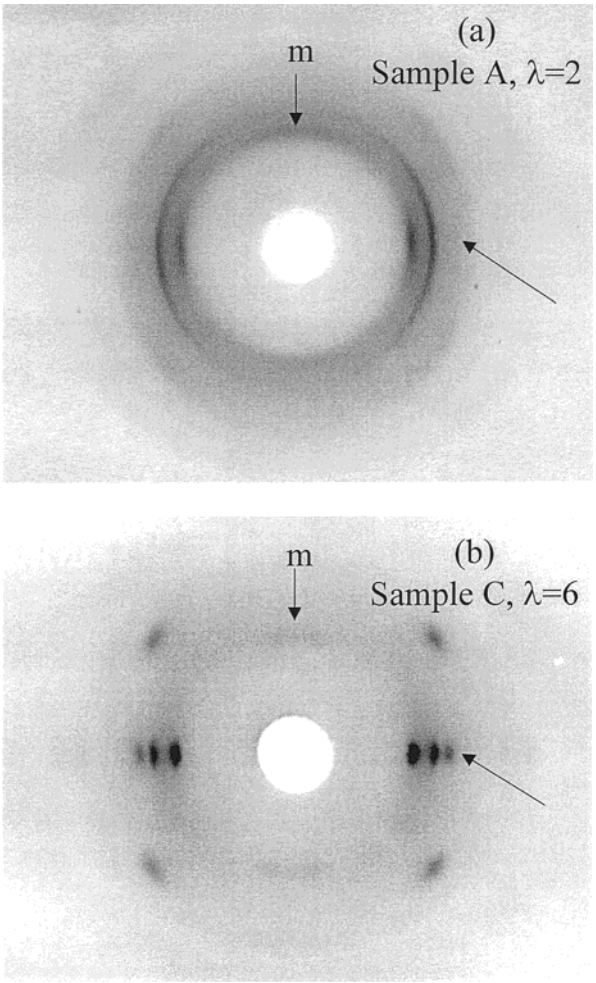

Figure 2. X-ray fiber diffraction patterns of two samples of elastomeric, poorly isotactic polypropylene obtained by stretching films quenched from the melt at different draw ratio λ: (a) sample A, $\lambda = 2$; (b) sample C, $\lambda = 6$. The patterns are recorded keeping the fiber samples under tension. The arrows close to the equator indicate in part a the $(117)_\gamma$ reflection, typical of the γ form, and in part b the $(130)_\alpha$ reflection typical of the α form. The arrow labeled with "m" indicates in part a the nearly meridional $(111)_\gamma$ reflection, typical of the γ form, and in part b the contribution of the $(110)_\alpha$ reflection on the meridian probably due to the presence of a non-negligible amount of daughter lamellae tilted ≈81° with respect to the parent lamellae and/or to the presence of crystalline domains still ordered as in the γ form (see the text).

sample A is crystallized in a modification very close to the γ form of iPP.

For sample C, the observed reflections correspond to those of the α form (see Table 3). This sample is therefore crystallized in modifications close to the α form of iPP, the crystallites being preferentially oriented with the chain axes parallel to the stretching direction. Also in these cases, a nearly meridional reflection on the first layer line is present, probably due to the presence of a non-negligible amount of daughter lamellae tilted ≈81° with respect to the parent lamellae, (which are generally observed in uniaxially oriented specimens of iPP crystallized in the α form)[6−9] and/or to the presence of crystalline domains still ordered as in the γ form.

The X-ray diffraction profiles collected with the automatic diffractometer along the equator and the first layer line for samples A ($\lambda = 2$), B ($\lambda = 4$), and C ($\lambda = 6$), after the subtraction of the amorphous contribution are reported in Figure 3, parts a, a′, b, b′, c, and c′.

Table 3. Miller Indices, Observed Bragg Distances (d_{obs}), Bragg Angles ($2\theta_{obs}$), and Intensities (I_{obs}) in the X-ray Fiber Diffraction Pattern of Samples A of Figure 2a and of sample C of Figure 2b

Sample A

$(hkl)_\gamma$	d_{obs} (Å)	$2\theta_{obs}$ (deg)	I_{obs}[a]
Equator			
111	6.42	13.8	s
008	5.51	16.7	ms
117	4.44	20.0	w
First Layer Line			
111	≈6.42	≈13.8	s
202, 026	4.18	21.3	ms

Sample C

$(hkl)_\alpha$	d_{obs} (Å)	$2\theta_{obs}$ (deg)	I_{obs}[a]
Equator			
110	6.25	14.2	s
040	5.20	16.8	ms
130	4.80	18.4	m
First Layer Line			
110 (tilted lamellae)	≈6.42	13.8	w
111, $\bar{1}$31, 041	4.18	21.3	s

[a] s = strong, ms = medium strong, m = medium, w = weak.

Samples B and C show very similar X-ray diffraction patterns. As already observed in Figure 2, the third strong equatorial reflection occurs at $\xi = 0.226$ Å^{-1} for sample A (indexed $(117)_\gamma$, Figure 3a) typical of the γ form, at $\xi = 0.210$ Å^{-1} for samples B and C (indexed $(130)_\alpha$, Figure 3b,c) typical of the α form.

Figure 4 plots the X-ray diffraction intensity measured as a function of the azimuthal diffraction angle χ, at fixed values of the 2θ diffraction angle, corresponding to the $(111)_\gamma$ reflection for sample A ($d = 6.40$ Å, Figure 4a) and to the $(110)_\alpha$ reflections for samples B and C ($d = 6.25$ Å, Figure 4, parts b and c, respectively), after subtraction for a horizontal baseline. The X-ray diffraction azimuthal profiles are resolved into four components: (i) two strong symmetrical peaks with maxima on the equator at $\chi = +90$ and $-90°$ (only half of these components are reported in the figure) and (ii) two additional peaks with maxima located at $\chi \approx +12°$ and $\chi \approx -12°$ (for sample A these two peaks are not well resolved, the dashed curves in Figure 4 indicate the two component of the broad peak). In the 2D X-ray diffraction patterns, the latter peaks are observed on the first layer line and are nearly meridional (see Figure 2, the reflections labeled with m); they are indexed as $(111)_\gamma$ for sample A (Figure 3a′ and Table 1) and $(110)_\alpha$ for samples B and C, for an *a* axis orientation (see Figure 3b′ and c′, respectively and Table 2). Notice that for γ crystals with the $a_\gamma b_\gamma$ diagonals of the orthorhombic unit cell oriented along the preferred (stretching) direction, the exact location of these maxima along the azimuthal profile, would correspond to $|\chi| \approx 12°$, as indeed observed in the case of sample A (Figure 4a); in the case of α crystals with chain axes tilted ≈81° with respect to the stretching direction, instead, these components would occur at $|\chi| \approx 16°-17°$. The observed maxima at $|\chi| = 12°$ in Figure 4, parts b and c, for samples B and C, respectively, are possibly explained with the presence of structural disorder, consisting in the presence of γ-like packing situations between adjacent bilayers in otherwise ordered domains of α form

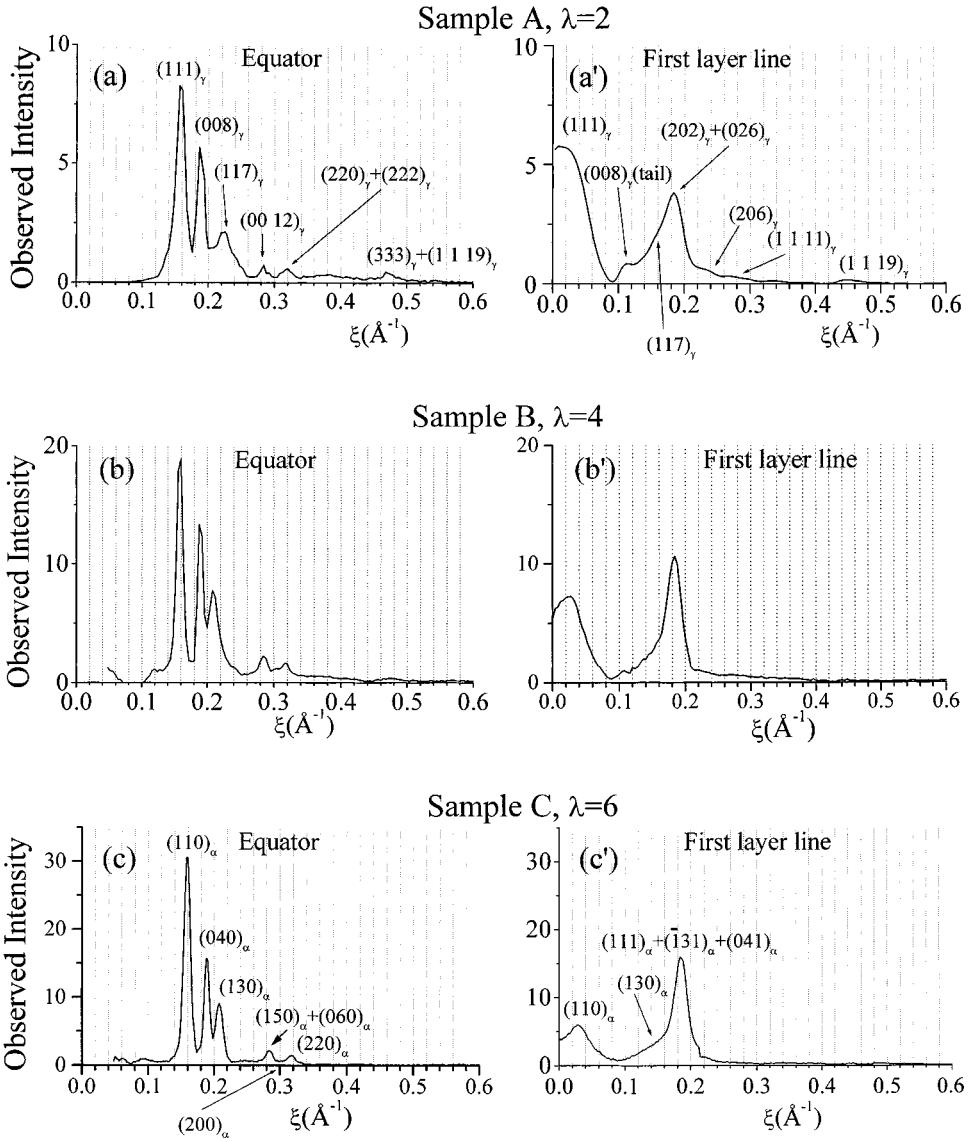

Figure 3. X-ray diffraction profiles collected with an automatic diffractomer along the equator and the first layer line as a function of the cylindrical coordinate ξ for samples A, $\lambda = 2$ (a, a′), B, $\lambda = 4$ (b, b′), and C, $\lambda = 6$ (c, c′) after subtraction of the amorphous contribution.

and implying a substantial coherent diffraction of differently oriented domains. As a matter of fact, the observed lack of intermediate preferred orientations of the crystalline domains between 0 and ≈81° in the 2D X-ray diffraction patterns of Figure 2, indicates a substantial coherence in the diffraction of these domains, as in the γ modification.

Calculation Method

The observed distribution of the X-ray diffraction intensities of samples A, B, and C, reported in Figure 3, does not match either those expected in the case of the pure γ form of iPP for sample A or those of the pure α form of iPP in the case of samples B and C and cannot be interpreted simply in terms of the sum of two independent contributions coming from the presence of different crystallites of the γ and α forms. The diffracted intensity may be interpreted assuming that disorder is present in the crystalline regions of our samples. The disorder leads consecutive bilayers of chains to face each other with the chain axes either parallel (like in the α form) or tilted ≈81° each other (like in the γ form) giving rise in otherwise ordered domains in the α or γ form, to a mixture at a molecular level, of the two polymorphs. However, the presence of small amounts of crystals in the α form for sample A, in the γ form for samples B and C, may not be excluded.

A possible model for a disordered arrangement of bilayers of chains present in the crystalline domains of our samples is reported in Figure 5. The disorder is imagined as originating from the random succession of bilayers along the direction b_α ($\equiv c_\gamma$) with chain axes parallel (as in the α form) or tilted ≈81° (as in the γ form) to each other. This disorder is not in contrast with a model of structural disorder already proposed in the literature to account for the X-ray powder diffraction patterns of some unoriented iPP samples[19] and appears reasonable in the light of the close structural analogies between the α and γ forms.

In this section, a method is derived for the calculation of the X-ray diffraction intensity distribution accounting for the presence of structural disorder of the kind shown in Figure 5. The calculated intensity (I_c) to be compared with the experimental X-ray diffraction intensity collected along the layer lines for our samples is evaluated by integrating in the reciprocal space the intensity

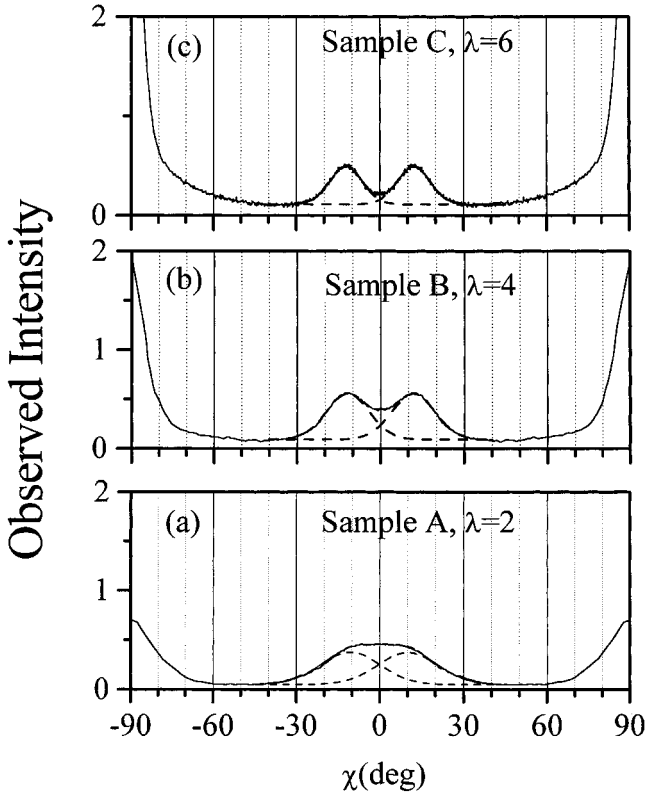

Figure 4. X-ray diffraction azimuthal scans at d = 6.40 Å, for sample A and at d = 6.25 Å for samples B and C, corresponding to the $(111)_\gamma$ and $(110)_\alpha$ reflections, respectively. The dashed lines represent the resolved Gaussian components of the reflections.

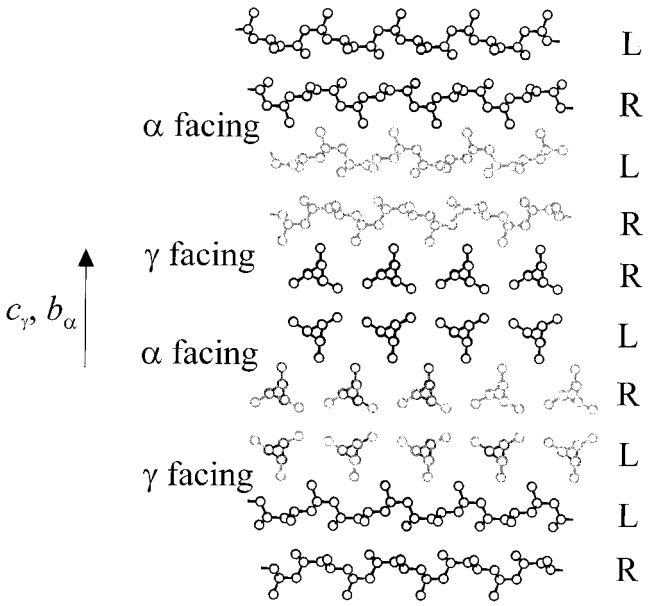

Figure 5. Model of the α/γ disorder occurring in the intermediate modifications of iPP between the α and the γ forms. Consecutive $a_\gamma b_\gamma$ ($a_\alpha c_\alpha$) bilayers of chains are stacked along c_γ (b_α) with the chain axes either parallel, making a α-like facing, or tilted ≈81° each other making a γ-like facing situation. R and L identify rows of all right- and all left-handed chains, respectively.

function $I(\xi,\zeta,\varphi)$, along circles with a constant value of the cylindrical coordinate ξ with $\zeta = n/c$ (n is an integer number and c the fiber axis identity period) and φ the angle between ξ and a^*. The line integral in these coordinates system is given by the equation

$$I_c = \frac{1}{2\pi}\int_0^{2\pi} I(\xi,\zeta,\varphi)\, d\varphi \qquad (1)$$

I_c is evaluated for domains of iPP chains ordered as in the structural models proposed for the α and the γ polymorphs of iPP as well as for disordered domains as shown in Figure 5. The X-ray diffraction intensity distribution in the fiber diagrams is strongly influenced not only by the amount of disorder in the stacking along c_γ (b_α) of $a_\gamma b_\gamma$ ($a_\alpha c_\alpha$) bilayers of chains, but also by the relative amount of the bilayers with the chain axes pointing along the draw direction, assumed to be parallel to the [110] or [$\bar{1}$10] lattice directions for the γ form (see Figure 6) or to c_α for the α form. For instance, the pure γ form domains preferentially oriented with the [110] or [$\bar{1}$10] lattice directions of the orthorhombic unit cells parallel to the fiber axis would necessarily imply that 50% of the bilayer point with the chain axes parallel, 50% with the chain axes tilted ≈81° to the preferred (draw) direction. On the other hand, α ordered domains could be, at least in principle, oriented with the chain axes either parallel, or nearly normal to the fiber axis direction. Finally, inclusion of a certain amount of α−γ disorder in the stacking of bilayers along the c_γ or b_α axis direction can imply several different distributions of the chain axes orientation in the two directions tilted ≈81° each other. Hence, our modeling should necessarily include these effects. To this aim, the calculations of the intensity function $I(\xi,\zeta,\varphi)$ was derived from a general method given by Allegra[20] as follows.

Without loss of generality, with reference to the orthorhombic unit cell of the γ form, let the labels 1, 2, and 3 identify the [110], [$\bar{1}$10], and [001] lattice directions (nearly equivalent to the [001], [100], and [010] lattice directions of the α form). With reference to Figure 6, let $\mathbf{v}_1(\approx\mathbf{c}_\alpha) = \mathbf{a}_\gamma + \mathbf{b}_\gamma/2$, $\mathbf{v}_2$ ($\approx\mathbf{a}_\alpha$) $= \mathbf{a}_\gamma - \mathbf{b}_\gamma/2$ and $\mathbf{v}_3$ ($\approx 2\mathbf{b}_\alpha$) $= \mathbf{c}_\gamma$ with moduli $v_1 = v_2 = 6.55$ Å and $v_3 = 42.41$ Å The labels 1 and 2 identify bilayers of iPP chains with the axes pointing along the lattice directions 1 and 2. A bilayer of kind 1 (2) may be thought as obtained by the regular repetition of a couple of enantiomorphous iPP helices (for clarity only one helix of this couple is shown in Figure 6) along the lattice direction 2 (1), through the translation vector $\mathbf{v}_2$ ($\mathbf{v}_1$); the repeating motif may be identifyied with the carbon atoms in one turn of two enanthiomorphic helices (18 atoms in total), repeating along the lattice direction 1 (2), through the translation vector $\mathbf{v}_1$ ($\mathbf{v}_2$). Let p_{ij} (i, j = 1, 2) be the conditional probabilities where a bilayer of kind i is followed along the direction 3 by a bilayer of kind j. At the interface of adjacent bilayers, local arrangements of the chains as in the α or γ form are obtained for $i = j$ or $i \neq j$, respectively. The origin of the local frame associated with each bilayer was chosen so that the translation vectors $\boldsymbol{t}_{ij}$ relating adjacent bilayers piled along the direction 3 (bilayer i followed by bilayer j) are $\mathbf{t}_{11} = \mathbf{v}_2/2 + \mathbf{v}_3/4$, $\boldsymbol{t}_{22} = \mathbf{v}_1/2 + \mathbf{v}_3/4$, $\boldsymbol{t}_{12} = \mathbf{v}_3/4$, and $\boldsymbol{t}_{21} = \mathbf{v}_1/2 + \mathbf{v}_2/2 + \mathbf{v}_3/4$. The number of independent conditional probabilities are only 2, since the following relations hold true: $p_{11} + p_{12} = 1$ and $p_{22} + p_{21} = 1$. The regular stacking of bilayers of kind 1 (or 2) along the direction 3 gives rise to ordered domains with the chains packed according to the structural model proposed for the α form of iPP, all the chain axes being parallel (or ≈81° tilted) to the draw direction, the unit cell parameters being only slightly modified with respect

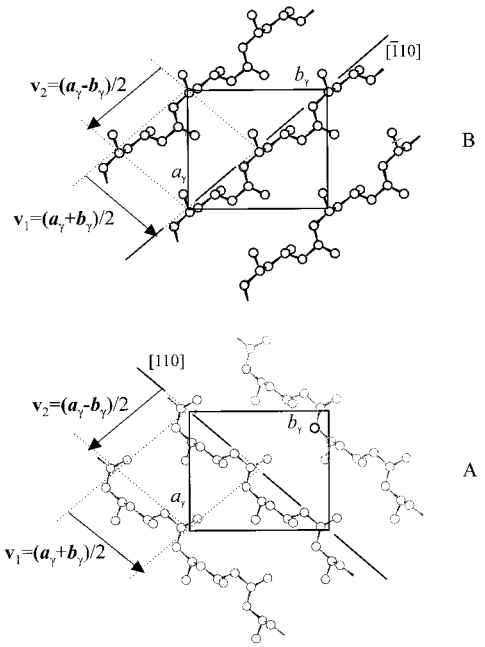

Figure 6. Orthorhombic unit cell of the γ form,[11] in a projection perpendicular to the [001] (i.e., $\equiv c_\gamma$) lattice direction. The chains are half parallel to the [110] lattice direction, half parallel to the [$\bar{1}$10] lattice direction, the two direction making an angle of 98.6°.

to those of ref 15. The regular alternation of bilayers of kind 1 and 2, instead, gives rise to domains ordered as in the γ form of iPP, and correponds to set $p_{12} = p_{21} = 1$. It is worth noting that the setting $p_{11} = p_{22} = 1$ corresponds to a 1:1 mixture of α-ordered domains with chain axes either parallel or ≈81° tilted to the draw direction, diffracting incoherently. The fraction of bilayers of kind 1 (i.e., with chain axes parallel to the preferred (stretching) direction), $f_{||}$ for the assumed statistical model is given by $f_{||} = (1 - p_{22})/(2 - p_{11} - p_{22})$ (hence, $f_\perp$, i.e., the fraction of bilayers with the chain axes tilted ≈81 to the fiber axis direction, is equal to $f_\perp = 1 - f_{||} = (1 - p_{11})/(2 - p_{11} - p_{22})$). The other relevant parameter, in our statistical model, is the fraction of facing situations between adjacent bilayers of kind α or γ, f_α, and $f_\gamma = 1 - f_\alpha$, respectively: $f_\alpha = f_{||}p_{11} + f_\perp p_{22}$. A Bernoulli type distribution of the size of the crystallites along directions 1, 2, and 3 is supposed, the symbols L_1, L_2, and L_3. denoting the apparent average length along the three directions, respectively.[21] Following the treatment given by Allegra[20] $I(\xi,\zeta,\varphi)$ is given by the following formula

$$I(\xi,\varsigma,\varphi)/\langle N\rangle = 2\, Real[\mathbf{VF}(\mathbf{E} - \mathbf{Q})^{-1}\tilde{\mathbf{V}}^*] - f_1 V_1 V_1^* - f_2 V_2 V_2^* \quad (2)$$

where $\langle N\rangle$ is the average number of bilayers piled along the direction 3 for the given Bernoulli type distribution of the size of the crystallites; **V** is the row vector whose elements are the structure factors of the two kinds of bilayers, $|V_1\ V_2|$; $\tilde{\mathbf{V}}^*$ is the column vector of the corresponding complex conjugates; **F** is the diagonal matrix:

$$\mathbf{F} = \begin{vmatrix} f_{||} & 0 \\ 0 & f_\perp \end{vmatrix} \quad (3)$$

Q is the matrix

$$\mathbf{Q} = \{1 - \exp[-2c/(4L_3)]\} \begin{vmatrix} p_{11}\exp(-2\pi i\mathbf{t}_{11}\cdot\mathbf{s}) & p_{12}\exp(-2\pi i\mathbf{t}_{12}\cdot\mathbf{s}) \\ p_{21}\exp(-2\pi i\mathbf{t}_{21}\cdot\mathbf{s}) & p_{22}\exp(-2\pi i\mathbf{t}_{22}\cdot\mathbf{s}) \end{vmatrix} \quad (4)$$

with **s** the reciprocal scattering vector, 2(sin θ)/λ. Finally, **E** is the 2 × 2 unit matrix.

The fractional coordinates of the atoms in the repeating motif in the bilayers, used in all the reported calculations, were deduced from those reported in ref 11 for the γ fom. The up/down disorder was considered in the calculations, the structure factors V_1 and V_2 in eq 2 being average values evaluated assuming each lattice site to be occupied with equal probability by chains up and down.

The apparent size of the crystallites along the direction 3(L_3) was deduced, applying Scherrer's formula, from the half-height width of the $(008)_\gamma$ (for sample A) and $(040)_\alpha$ (for samples B and C) diffraction peaks in the experimental profiles of Figure 3a−c; it is equal to ≈40 Å for sample A and close to 60 Å for samples B and C. The values of L_1 (assumed equal to L_2 in all the calculations), have been deduced from the half-height width of the equatorial peaks, with indices $(111)_\gamma$ and $(117)_\gamma$ for sample A, and $(110)_\alpha$ and $(130)_\alpha$ for samples B and C; they correspond to $L_1 = L_2 = 80$, 100, and 120 Å for samples A, B, and C, respectively. As a final remark, we notice that the apparent half-height width of the X-ray diffraction peaks along the first layer line of the three examined samples (see Figure 3, parts a′, b′, and c′) may be increased by the not perfect parallelism between the chain axes belonging to different ordered domains and the preferred (draw) direction in the experimental case: since this effect is not included in the calculations,[22] the calculated profiles along the first layer line, will appear narrower than the experimental ones.

Results of the Calculations

1. X-ray Diffraction Calculations for Limit Fully Oriented Polymers: α and γ Forms and the Completely Statistically Disordered Case. The calculated X-ray diffraction profiles along the equator and the first layer line as a function of ξ for ordered domains with chains packed according to the model structures proposed for the pure α and the pure γ forms of iPP and in the completely statistically disordered case, are reported in Figure 7. For the pure α form, two cases are considered: (i) the ordered domains are oriented with the chain axes parallel to the draw direction ($f_\alpha = 1$, $f_{||} = 1$, Figure 7c, c′); (ii) the ordered domains with the chain axes tilted 81.4° with respect to the fiber axis direction ($f_\alpha = 1$, $f_\perp = 1 - f_{||} = 1$; Figure 7b,b′). For the γ form, the domains are supposed to be oriented with the [110] (or [$\bar{1}$10]) axis direction (i.e., one of the two $a_\gamma b_\gamma$ diagonals in the orthorhombic unit cell) parallel to the draw direction ($f_\gamma = 1 - f_\alpha = 1$, $f_{||} = f_\perp = 0.5$; Figure 7a,a′). Finally, the calculations have been performed also for crystalline domains including statistical disorder of the kind of Figure 5; the case with $f_\alpha = f_\gamma = 0.5$, $f_{||} = f_\perp = 0.5$ is plotted in Figure 7d as an example. In all the calculations the values of $L_1 = L_2$ and L_3 are fixed equal to 1000 and 500 Å, respectively. For comparison, in the disordered case, the calculations for domains having dimensions of the same order of magnitude as those experimentally detected, i.e., $L_1 = L_2 = 100$ Å and $L_3 = 50$ Å, are also reported.

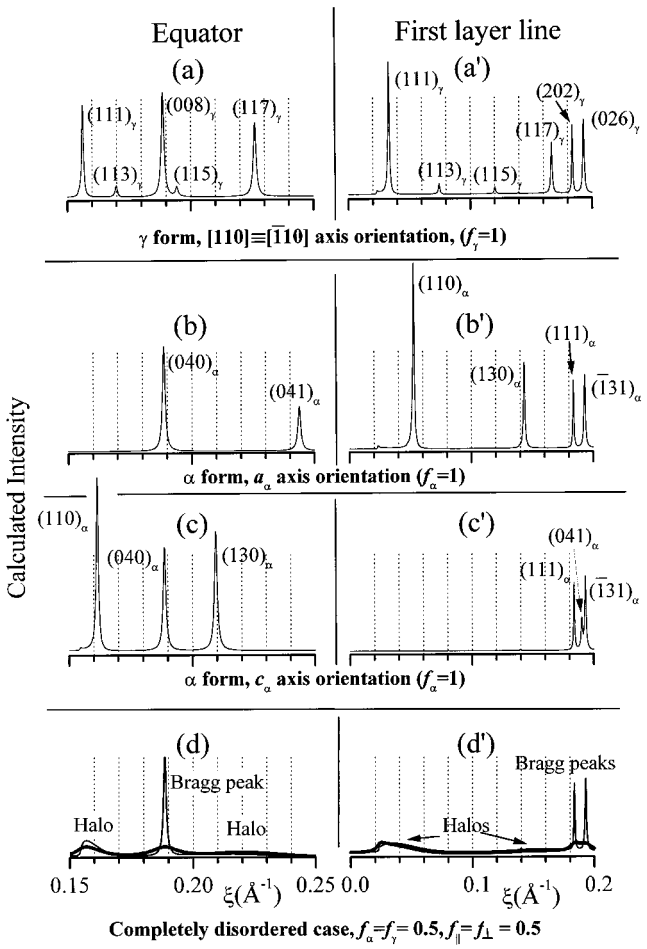

Figure 7. Calculated X-ray diffraction profiles along the equator and the first layer line, as a function of the cylindrical coordinate ξ, for the ordered α form, with chain axes parallel to the fiber axis direction (c, c′, $f_\alpha = 1$, $f_{||} = 1$); for the ordered α form with the chain axes tilted ≈81° to the fiber axis direction (b, b′, $f_\alpha = 1$, $f_{||} = 0$); for the ordered γ form with the diagonals $\mathbf{a}_\gamma + \mathbf{b}_\gamma$ or $\mathbf{a}_\gamma - \mathbf{b}_\gamma$ of the orthorhombic unit cell parallel to the fiber axis direction (a, a′, $f_\gamma = 1 - f_\alpha = 1$, $f_{||} = 0.5$); for a disordered domain comprising α/γ structural disorder of the kind shown in Figure 5, with $f_\alpha = f_\gamma = 0.5$ and $f_{||} = f_\perp = 0.5$ (d, d′). The calculations have been performed for domains having dimensions $L_1 = L_2 = 1000$ Å, $L_3 = 500$ Å; in d and d′ the thick line is relative to $L_1 = L_2 = 100$ Å, $L_3 = 50$ Å. The $(hkl)_\gamma$ reflections of the orthorhombic unit cell of the γ form and the $(hkl)_\alpha$ reflections of the monoclinic unit cell of α form are indicated.

The calculated X-ray diffraction profiles in the ordered forms show close analogies. For instance, for the γ form, the $(008)_\gamma$ reflection on the equator (Figure 7a) and the $(202)_\gamma$ and $(026)_\gamma$ reflections on the first layer line (Figure 7a′) are equivalent, not only as far as the position (see Tables 1 and 2) but also for the intensity to the $(040)_\alpha$, $(111)_\alpha$, and $(\bar{1}31)_\alpha$ reflections in the pure α form, whatever the orientation of the chains (Figure 7b,b′,c,c′). The most relevant differences between the calculated patterns of the ordered forms are in the positions of the first and the third strongest equatorial reflection occurring at $\xi = 0.160$ and 0.210 Å^{-1} in the α form, c_α axis orientation, ($(110)_\alpha$ and $(130)_\alpha$, Figure 7c) at 0.156 and 0.226 Å^{-1} in the pure γ form ($(111)_\gamma$ and $(117)_\gamma$, Figure 7a). Moreover, along the first layer line at low ξ values, a strong diffraction peak is apparent for the pure γ form at $\xi \approx 0.030$ Å^{-1} ($(111)_\gamma$ reflection, Figure 7a′) and for the α domains with an a_α axis orientation at $\xi \approx 0.045$ Å^{-1} ($(110)_\alpha$ Figure 7b′) whereas the diffraction intensity in this ξ range would be calculated nearly zero for α domains with a c_α axis orientation, (Figure 7c′). For α domains c_α axis oriented, the integrated intensities of the first three strongest equatorial reflections (i.e., $(110)_\alpha$, $(040)_\alpha$, and $(130)_\alpha$) are in the ratio1.3:1:1.15 (Figure 7c), whereas in the case of the tilted α lamellae they are in the ratios 0:1:0 (Figure 7b); finally for γ domains oriented with the $a_\gamma b_\gamma$ diagonals of the orthorhombic unit cell along the preferred direction, the first three strongest equatorial reflections (i.e., $(111)_\gamma$, $(008)_\gamma$, and $(117)_\gamma$) have calculated intensities in the ratios 0.58:1:0.75 (Figure 7a).

The intensity and the position of the reflections with Miller indices $(008)_\gamma$, $(202)_\gamma$, and $(026)_\gamma$, (Figure 7a,a′), corresponding to the $(040)_\alpha$, $(111)_\alpha$ and $(131)_\alpha$ in the α form (Figure 7b,b′,c,c′), remain unaffected even in the presence of structural disorder of the kind shown in Figure 5 and/or whatever the relative amount of different crystalline phases present in a given sample (eventually comprising the presence of tilted α domains). The intensity of the reflections not belonging to this class, would be strongly affected by the presence of disorder and/or by the kinds and the relative amounts of the phases present in a given sample, instead. For domains having large dimensions these reflections would remain strong and sharp for a mixture of different forms and become broad and flat (halos) for domains including α/γ structural disorder (see Figure 7d,d′, thin line). For scattering domains having small dimensions, instead, all the reflections appear rather broad, and it is more difficult to distinguish between those whose positions, shapes, and intensities are left unchanged and those whose intensity is modified because of the presence of disorder and/or a mixture of different forms is present (see Figure 7d, thick line). Since the average size of the crystallites of samples A, B, and C is not large, the analysis of the structural features (presented in the next section) will be performed through a direct comparison of the experimental X-ray diffraction data with those calculated for suitable model structures

2. X-ray Diffraction Calculations for Mixtures of α and γ Domains and for Disordered Model Structures. Comparison with the Experimental Data. The experimental X-ray diffraction profiles for sample A collected along the equator and the first layer line of Figure 3a,a′ are reported in Figure 8, parts d and d′, as a function of ξ, after the *Lp* correction and compared with the profiles calculated for various structural models. The following limiting cases are considered: the pure γ form (Figure 8c,c′); a mixture of crystalline domains 25% ordered as in the α form and 75% as in the γ form, scattering incoherently, the α domains being supposed to be all identically oriented along the preferred (stretching) direction (Figure 8b,b′); disordered domains with $f_\gamma = 1 - f_\alpha = 0.75$, and $f_{||} = 0.625$ (Figure 8a,a′). For the patterns a and a′ the α portions in the domains are all assumed oriented with the chain axes parallel to the preferred direction (i.e., $f_{||} = f_\gamma/2 + f_\alpha$). In all the calculations the values of $L_1 = L_2$ and L_3 are fixed equal to 80 and 40 Å, respectively. From this comparison, it is possible to establish that sample A is mostly crystallized in the γ form, but not in the pure γ form (Figure 8c,c′). To account for the relative intensities of the first three most intense equatorial reflections, indeed, a partial amount of packing situations as in the α form, should be present. The profiles b and b′, calculated in the hypothesis that a mixture of α and γ

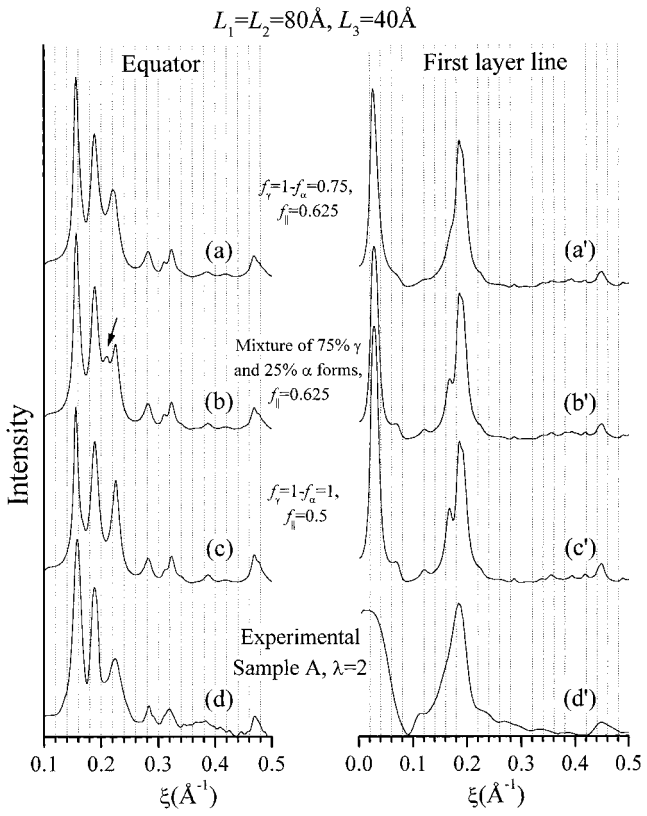

Figure 8. Comparison of the experimental X-ray diffraction profiles of sample A of Figure 3a, a′ after the *Lp* correction (d, d′) with those calculated along the equator and the first layer line as a function of the cylindrical coordinate ξ, for the pure γ form (c, c′, $f_\gamma = 1$, $f_{||} = 0.5$); mixtures of domains 25% in the α, 75% in the γ form, with $f_{||} = 0.625$ (b, b′); for disordered $\alpha-\gamma$ domains of the kind of Figure 5 with $f_\gamma = 1 - f_\alpha = 0.75$, and $f_{||} = 0.625$ (a, a′). All the calculations have been performed for domains having dimensions $L_1 = L_2 = 80$ Å, $L_3 = 40$ Å.

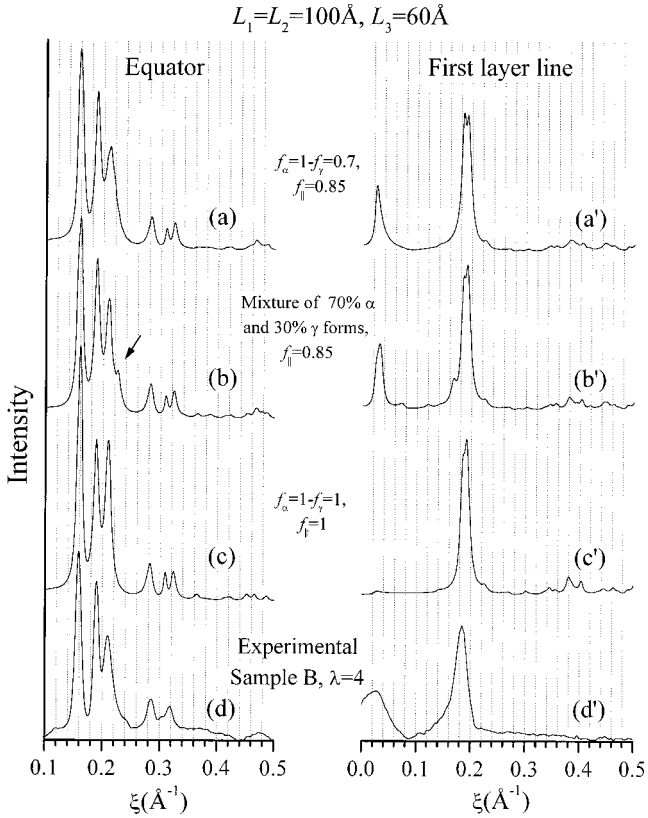

Figure 9. Comparison of the experimental X-ray diffraction profiles of sample B of Figure 3b,b′ after the *Lp* correction (d, d′) with those calculated along the equator and the first layer line as a function of the cylindrical coordinate ξ, for the pure α form (c, c′, $f_\alpha = 1$, $f_{||} = 1$); mixtures of domains 30% in the γ, 70% in the α form, with $f_{||} = 0.85$ (b, b′); for disordered $\alpha-\gamma$ domains of the kind of of Figure 5 with $f_\alpha = 1 - f_\gamma = 0.70$ and $f_{||} = 0.85$ (a, a′). All the calculations have been performed for domains having dimensions $L_1 = L_2 = 100$ Å, $L_3 = 60$ Å.

crystals diffracting incoherently are present in the sample, give a better agreement with the experimental profiles, but pattern b presents a non-negligible maximum at $\xi = 0.210$ Å^{-1} corresponding to the $(130)_\alpha$ reflection (peak marked with an arrow), which is absent in the experimental profile; also, in curve b, the third equatorial peak is still too sharp compared to the experimental one. The best agreement with the experimental data is obtained in the hypothesis that the $\alpha-\gamma$ mixing occurs at a molecular level, thus generating structural disorder of the kind shown in Figure 5 (compare profiles a and a′ with the experimental ones, d and d′, in Figure 8) although the presence of small amounts of α crystals scattering incoherently with respect to the γ domains may not be excluded.

It is worth noting that in sample A the bilayers of chains in the α regions of the disordered crystals are probably arranged with the chain axes preferably parallel to the stretching direction rather than ≈81° tilted to it; in fact, the calculated relative intensity of the first equatorial reflection $(111)_\gamma$ with respect to the intensity of the $(008)_\gamma$ reflection decreases with decreasing $f_{||}$ and becomes already too low with respect the experimental data, when the orientational distribution along the two axes 81° tilted each other is assumed to be the same (i.e., $f_{||} = 0.5$; the calculated profiles for this case are not reported here). This result is reasonable, since our sample is subject to a mechanical stress-field which tend to align the chain axes parallel to the draw direction. From this analysis it is possible to establish that sample A is crystallized in a disordered modification intermediate between the γ and the α forms, with ≈75% of the bilayers facing each other as in the γ form, the remaining 25% being arranged as in the α form, the fraction of bilayers with chain axes pointing preferentially along the draw direction being on the order of ≈60%.

The experimental X-ray diffraction profiles for samples B and C collected along the equator and the first layer line of Figure 3, parts b, b′ and c, c′, are reported in Figures 9d,d′ and 10d,d′, respectively, as a function of ξ, after the *Lp* correction and compared with the profiles calculated for various structural models. More precisely, in both figures, profiles c and c′ are relative to the pure α form in the c_α axis orientation, profiles b and b′ to mixtures of α and γ forms in the ratios 70:30 (Figure 9) and 80:20 (Figure 10), in the hypotheses that all α domains are oriented with the chain axes parallel to the stretching direction. Finally, profiles a, a′ are relative to disordered crystals, like that of Figure 5, where the $\alpha-\gamma$ mixing is assumed to occur at a molecular level, i.e., $f_\alpha = 0.7$, $f_{||} = 0.8$ (Figure 9a,a′) and $f_\alpha = 0.8$, $f_{||} = 0.9$ (Figure 10a,a′). In all the calculations the values of $L_1 = L_2$ and L_3 are fixed equal to 100 and 60 Å, respectively, in Figure 9, and to 120 and 60 Å, respectively, in Figure 10.

From this comparison, it is possible to establish that samples B and C are both crystallized in modifications very close to the α form of iPP, with the chain axes

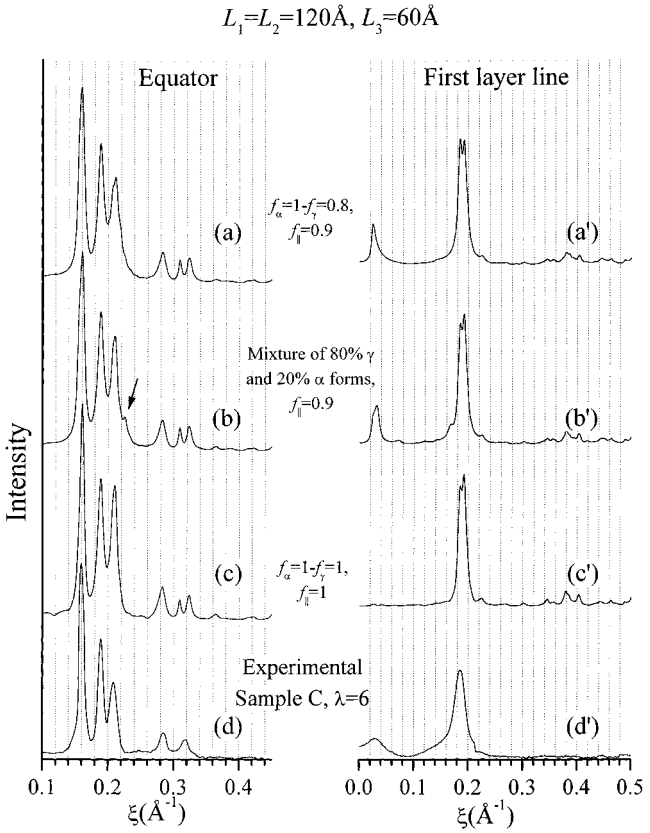

Figure 10. Comparison of the experimental X-ray diffraction profiles of sample C of Figure 3c,c′ after the *Lp* correction (d, d′) with those calculated along the equator and the first layer line as a function of the cylindrical coordinate ξ, for the pure α domain (c, c′, $f_\alpha = 1$, $f_{||} = 1$); mixtures of domains 20% in the γ, 80% in the α form, with $f_{||} = 0.9$ (b, b′); for disordered α−γ domains of the kind of Figure 5, with $f_\alpha = 1 - f_\gamma = 0.80$ and $f_{||} = 0.9$ (a, a′). All the calculations have been performed for domains having dimensions $L_1 = L_2 = 120$ Å, $L_3 = 60$ Å.

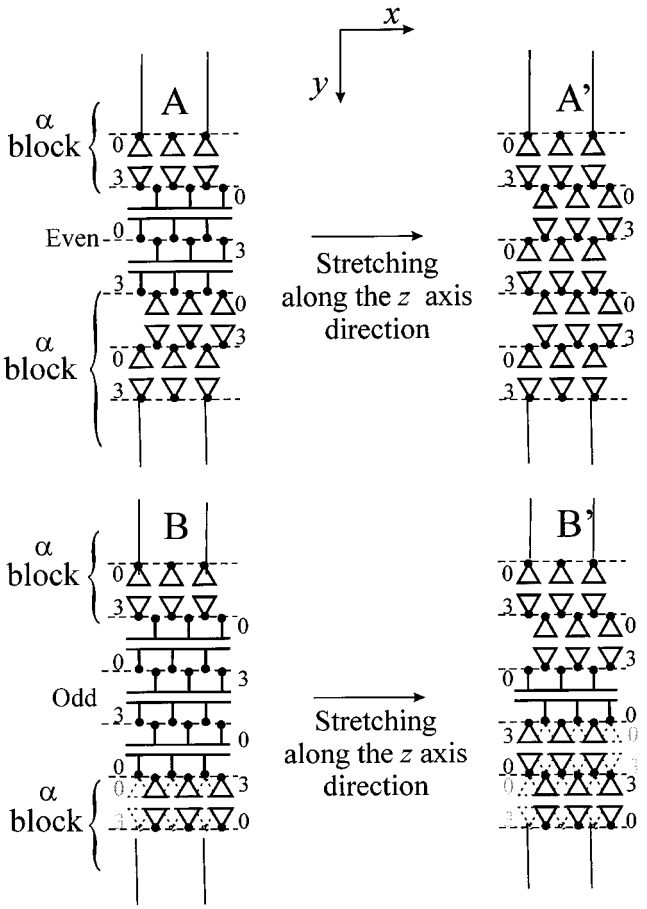

Figure 11. Schematic model showing the effect of the stretching on our sample. Two α blocks of iPP with chain axes oriented parallel to the *z* axis (stretching) direction joined by a number (*n*) of bilayers with the chain axes tilted by ≈81° to the *z* axis: (A) *n* = even (=2) and (B) *n* = odd (=3). The horizontal dashed lines delimit adjacent bilayers. The numbers indicate, in c_α/6 units, the fractional coordinate *z* of the methyl groups placed at the interface between adjacent bilayers (filled balls). In B the two α blocks result out of phase $^1/_2a_\alpha + {}^1/_2c_\alpha$ with respect to a fully ordered α domain (the dashed triangles indicate the positions occupied by the chains of the lower block, if the two domains were in phase, the numbers in gray being the *z* fractional coordinates of the methyl groups). Upon stretching, the fraction of chains with the axes parallel to *z* increases: a fully ordered α domain is obtained with *n* even (A′); at least a single defective bilayer, with the chain axes ≈81° tilted to the stretching direction, is left embedded between the two α domains, when *n* is odd (B′).

preferably oriented along the stretching direction, but not in the pure α form. In fact, the ratio between the intensities of $(130)_\alpha$ and $(040)_\alpha$ reflections is calculated too high for a pure α form (Figure 9c and 10c) with respect to the experimental ones. Moreover, a non-negligible diffraction maximum centered at $\xi = 0.022$ Å^{-1} is apparent on the first layer line of the experimental patterns of both samples, which is absent in the diffraction profiles of the pure α form in the *c*-axis orientation. It is worth noting that these experimental features may not be fully ascribed to the presence in the sample of branching lamellae (i.e., α domains in the a_α axis orientation), because in this hypothesis a non-negligible diffraction maximum on the first layer line centered at $\xi = 0.043$ Å^{-1} rather than at 0.022 Å^{-1}, would appear (see the Figure 7 and the discussion in the previous subsection). To account for the experimental X-ray diffraction patterns of samples B and C, a partial amount of packing situations as in the γ form, should be present. The profiles b and b′ of Figures 9 and 10 calculated for mixtures of α and γ domains diffracting incoherently, give a better agreement with the experimental profiles, but for the presence in the profiles of Figure 9b and 10b of a shoulder at $\xi = 0.226$ Å^{-1}, (arrowed in the figures, corresponding to the $(117)_\gamma$ reflection) which is absent in the experimental profiles. As for sample A, the best agreement with the experimental data is obtained in the hypothesis that the α−γ mixing occurs at a molecular level (see Figure 5), possibly with the chain axes in the α portions all identically oriented parallel to the stretching direction (compare profiles a, a′ with the experimental ones d, d′, in Figures 9 and 10), although the presence of small amounts of γ crystals as well as of α tilted lamellae scattering incoherently with respect to the α domains c_α-axis oriented, may not be excluded.

In conclusion, from the above analysis, it is possible to establish that also samples B and C result crystallized in disordered modifications intermediate between the α and γ forms, the fraction of bilayers facing each other like in the γ form being on the order of 30% for sample B, 20% for sample C and with a fraction of bilayers pointing with the chain axes ≈81° tilted to the stretching direction on the order of 10−20% in both samples.

This analysis indicates that stretching procedures of a poorly stereoregular PP sample, initially in modifica-

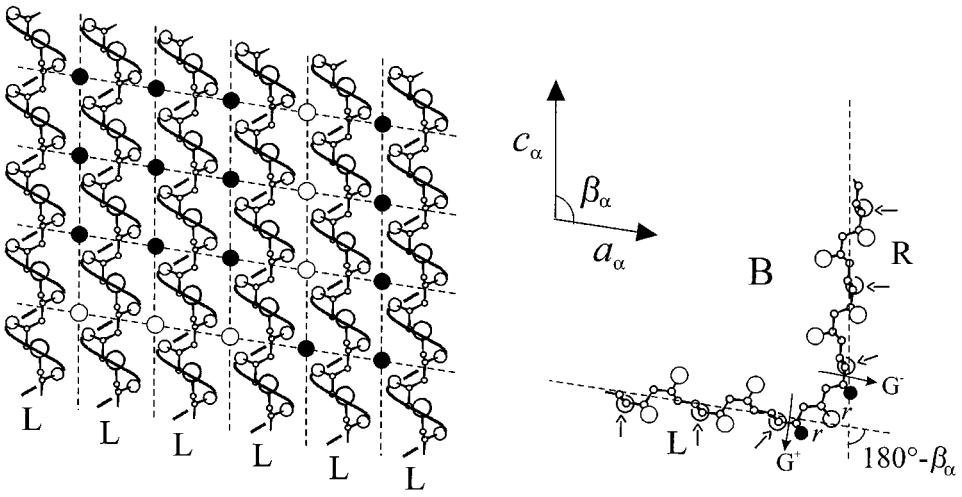

Figure 12. (A) Row of left-handed chains corresponding to half bilayer, in a projection containing the chain axes. The knots of the network of dashed lines, evidenced with the filled and empty circles, identify the positions occupied by the methyl groups of the chains belonging to the next adjacent bilayer. The adjacent bilayer may be arranged with the chains parallel to the vertical dashed lines, making a α-like facing, or parallel to the tilted dashed lines making a γ-like facing. (B) Helix reversal occurring in a stem of a isotactic polypropylene chain, pinned to a *rr* triad; the dihedral angles in the *rr* triad are in a nearly-trans conformation. The helical axes associated with the enanthiomorphous helical stems form and angle of ≈81°, and the methyl groups indicated by arrows in the figure are in register with the crystallographic positions indicated by the empty circles in part A. Symbols R and L stand for right- and left-handed helices. The bent chain, once arranged in the lattice A with the arrowed methyl groups in the positions of the empty circles, makes a α-like arrangement with the vertical stem of the chain and a γ-like arrangement with the tilted stem.

tions close to the γ form, lead to a gradual transformation to the α form, which is mechanically more stable. This transition occurs through a continuum of disordered modifications intermediate between the γ and the α forms. For instance, for sample C, which is drawn up to $\lambda = 6$, the fraction of bilayers arranged like in the γ form is not reduced to zero. Figure 11 plots a schematic model showing the effect of the stretching on our sample. Let us imagine two blocks of α form of iPP with chain axes oriented parallel to the stretching (*z*) direction joined by a number (*n*) of bilayers with the chain axes ≈81° tilted to it (the bilayers are delimited by the horizontal dashed lines): the two cases *n* even ($n = 2$) and odd ($n = 3$) are shown in Figure 11, parts A and B, respectively. The numbers indicate in $c_\alpha/6$ units the fractional coordinate *z* of the methyl groups placed at the interface between adjacent bilayers (filled balls). When *n* is odd (Figure 11B), the two α blocks result out of phase $^1/_2a_\alpha + {}^1/_2c_\alpha$ with respect to a fully ordered α domain (the chains of the lower block, would be placed in the positions indicated by the dashed triangles and shifted $^1/_2$ along c_α in a fully ordered α crystal). When *n* is even (Figure 11A) the two α block are arranged like in a fully ordered α crystal. Because of the application of an uniaxial stress, the fraction of chains with the axes parallel to the stretching direction increases. If *n* is even, a fully ordered α domain is obtained (Figure 11A′); if *n* is odd, at least a single defective bilayer, with the chain axes ≈81° tilted to the stretching direction, should be left embedded between the two α domains (Figure 11 B′), to obtain a low packing energy arrangement of the chains. As a result, while the number of chains with axes parallel to the draw direction increases, the number of interfaces with a γ-like arrengment is left unaltered when *n* is odd. Since f_γ is never reduced to zero, the fraction of ≈81° tilted bilayers, $f_\perp$, should be at least on the order of $f_\gamma/2$.

Conclusions

The polymorphic behavior of a novel, poorly stereoregular polypropylene sample ([*mmmm*] = 35%), prepared with a new C_2-symmetric zirconocene based catalytic system,[10] is investigated. This sample shows elastomeric properties. It is initially amorphous, but partially crystallizes upon aging. In the oriented material obtained by stretching the sample, the crystallites tend to assume a preferred orientation with the chain axes parallel to the draw direction. For low draw ratios (less than twice the initial length), crystalline modifications, very close to the γ form of iPP, are obtained. With an increase in the draw ratio, crystalline modifications, closer to the α form of iPP, are obtained. The comparison of the experimental X-ray diffraction profiles with those calculated for various model structures allows one to establish that the pure γ and the pure α forms are never reached. In all examined samples, indeed, a non-negligible amount of structural disorder is present. This disorder consists of the random succession of $a_\gamma b_\gamma$ ($a_\alpha c_\alpha$) bilayers of chains along the c_γ (b_α) axis direction with the chain axes parallel (like in the α form) or tilted 81° (like in the γ form) each to other. For the sample stretched at a low draw ratio, ≈75% of the bilayers possibly face each to other as in the γ form, and the fraction of bilayers with chain axes pointing preferentially along the draw direction is on the order of 60% (the remaing 40% being oriented with the chain axes tilted ≈81° to the draw direction). For the samples stretched at higher draw ratios, the fraction of bilayers facing each other like in the γ form is reduced to 20−30%, and only 10−15% of the bilayers remain oriented with the chain axes nearly normal to the draw direction. A continuum of disordered modifications, intermediate between the pure α and γ forms, exists.

Although the examined samples are always poorly crystalline, it remains to be established how such a

poorly stereoregular material, with a nearly random distribution of defects, can give crystalline domains with sizes on the order of several tens of angstroms along the various lattice directions. The possible inclusion in the crystalline domains of stereo defects and in particular those of the kind *mrrm*, which are the most frequent ones, on the order of 10%, in our sample,[10] is here discussed. It is worth noting that in a recent paper VanderHart et al.,[23] through ^{13}C NMR techniques for the solid state, provide evidences that in metallocene iPP samples, consisting of mixed amounts of α and γ crystallites, simple stereo *mrrm*-type defects have a concentration in the crystalline regions of about half of their overall concentration in the iPP chain.

Figure 12A plots a row of left-handed helices corresponding to half bilayer in a growing crystal (bilayer *i*th), in a projection containing the chain axes. The open and filled circles placed at the knots of the network of the dashed lines, identify the positions occupied by the methyl groups belonging to the chains of the next adjacent bilayer along b_α (bilayer $(i + 1)$-th). These chains may run with the axes either parallel to the vertical dashed lines, (making a α-like facing) or parallel to the dashed lines pointing along the a_α lattice direction, (making a γ-like facing). We recall that, corresponding to α-like interfaces, the chains are enanthiomorphous, while corresponding to γ-like interfaces the chains should be isomorphous (see Figure 1). An intermediate possibility is represented by the inclusion in the growing crystal of a bent chain, of the kind shown in Figure 12B. Figure 12B shows, as an example, a low conformational energy helix reversal in a chain of isotactic polypropylene, pinned to a *rr* configurational defect. The vertical stem is a right-handed $(TG^-)_n$ fully isotactic sequence connected to a left-handed $(G^+T)_n$ fully isotactic sequence through a *rr* triad. The dihedral angles close to the *rr* triad are in a nearly trans conformation. This defect would bend the chain by ≈81° and would lead the methyl groups arrowed in the figure in register with the lattice positions indicated by the empty circles in Figure 12A. In other terms, a chain stem like that of Figure 12B, containing a helix reversal once accommodated on a substrate of the kind shown in Figure 12A, with the arrowed methyl groups in the positions indicated by the empty circles, makes a α-like arrangement with a portion of the chain and a γ-like arrangement with the other portion. Because of this, part of the chains completing the $(i + 1)$-th bilayer could assume an orientations with the axes parallel to the a_α direction, the remaining part of chains an orientation parallel to the c_α lattice directions. Of course the next adjacent bilayer along b_α to the one including the defective chain, (bilayer $(i + 2)$-th), could be arranged, at least in principle, with the chain axes either parallel or ≈81° tilted to those belonging to the *i*th bilayer. Hence, the inclusion of defects of the kind shown in Figure 12B in the crystals, which is feasible at a low cost of conformational and packing energy, introduces a possible mechanism inducing in the studied sample the observed tendency to give rise to intermediate modifications between the α and γ forms.

Acknowledgment. The financial support by the Ministero dell'Università e della Ricerca Scientifica e Tecnologica PRIN 2000 is gratefully acknowledged. X-ray diffraction data were recorded with a Nonius MACH3 automatic diffractometer (Centro Interdipartimentale di Metodologie Chimico Fisiche, Universiy of Naples). We wish to thank Dr. L. Resconi, Basell Polyolefins of Ferrara, for providing the sample and for useful discussions.

References and Notes

(1) Brückner, S.; Meille, S. V.; Petraccone, V.; Pirozzi, B. *Prog. Polym. Sci.* **1991**, *16*, 361.
(2) Fisher, D.; Müllhaupt, R. *Macromol. Chem. Phys.* **1994**, *195*, 1433.
(3) Thormann, R.; Wang, C.; Kressler, J.; Müllhapt, R. *Macromolecules* **1996,** *29***,** 8425.
(4) Alamo, R. G.; Kim, M.-H.; Galante, M. J.; Isasi, J. R.; Mandelkern, L. *Macromolecules* **1999**, *32*, 4050.
(5) Awaya, H. *Polym. Lett.* **1966**, *4*, 127.
(6) Khoury, F. *Bull. Am. Phys. Soc.* **1964**, *9*, 275. Khoury, F. *J. Res. Nat. Bur. Stand.* **1966**, *A70*, 29.
(7) Sauer, J. A.; Morrow, D. R.; Richardson, G. C. *J. Appl. Phys.* **1965**, *36*, 3017.
(8) Padden, F. J., Jr.; Keith, H. D. *J. Appl. Phys.* **1966**, *37*, 4013.
(9) Lotz, B.; Wittmann, J. C. *J. Polym. Sci.: Polym. Phys.* **1986**, *24*, 1541.
(10) Balboni, D.; Moscardi, G.; Baruzzi, G.; Braga, V.; Camurati, I.; Piemontesi, F.; Resconi, L.; Nifant'ev, I. E.; Venditto, V.; Antinucci, S. *Macromol. Chem. Phys.* **2001**, *202*, 1780.
(11) Brückner, S.; Meille, S. V. *Nature* **1989**, *340*, 455.
(12) Meille, S. V.; Brückner, S.; Porzio, W. *Macromolecules* **1990**, *23*, 4114.
(13) IUPAC Commission on Macromolecular Numenclature. *Pure Appl. Chem.* **1981**, *53*, 733.
(14) Natta, G.; Corradini, P. *Nuovo Cimento Suppl.* **1960**, *15*, 40.
(15) Hikosaka, M.; Seto, T. *Polym. J.* **1973**, *5*, 111.
(16) Mencik, Z. *J. Mocromol. Sci. Phys.* **1972**, *B6*, 101.
(17) Auriemma, F.; Ruiz de Ballesteros, O.; De Rosa, C.; Corradini, P. *Macromolecules* **2000**, *23*, 8764.
(18) Auriemma, F.; De Rosa, C.; Resconi, L. Paper in preparation.
(19) Meille, S. V.; Philips, P. J.; Mzghani, K.; Brückner, S. *Macromolecules* **1996**, *29*, 795.
(20) Allegra, G. *Nuovo Cimento* **1961**, *21*, 786.
(21) Allegra, G.; Bassi, I. W. *Gazz. Chim. Ital.* **1980**, *110*, 437.
(22) Ruland, W. *Colloid. Polym. Sci.* **1977**, *15*, 1301.
(23) VanderHart, D. L.; Alamo, R. G.; Nyden, M. R.; Kim, M. H.; Mandelkern, L. *Macromolecules* **2000**, *33*, 6078.

MA0100504